International Journal of Power Trains, Volume 9, Issue 4, October 2020, pp. 265-288
DOI:10.1504/IJPT.2020.111227

How Suitable is Lithium-Sulfur Battery for Electric City Bus Application?

Victor Calvo-Serra, Abbas Fotouhi*, Mehdi Soleymani, and Daniel J. Auger

Advanced Vehicle Engineering Centre,
School of Aerospace, Transport and Manufacturing (SATM),
Cranfield University, Bedfordshire, MK43 0AL, UK
Email: victor.calvo.serra@gmail.com
Email: a.fotouhi@cranfield.ac.uk; abfotouhi@gmail.com
Email: m.soleymani@cranfield.ac.uk
Email: d.j.auger@cranfield.ac.uk
*Corresponding autor

Abstract
Lithium-sulfur (Li-S) battery is a promising technology that can be considered as an alternative energy storage system in automotive and aerospace applications due to its higher energy density, safety and potential lower price in mass production compared to the existing battery technologies in the market. This paper investigates application of a new prototype Li-S cell in an electric city bus using computer simulations. For this purpose, MATLAB/Simulink software has been employed and a vehicle model is built and simulated according to the specifications of available electric buses in London city. An equivalent circuit model is parameterized for the new Li-S cell based on experimental data. Battery pack sizing is then performed by considering the maximum required power and also the desirable energy stored in the pack based on the Millbrook London Transport Bus (MLTB) driving cycle. Furthermore, impact of the battery pack's mass on the vehicle's range is studied and Li-S technology is compared with two commercial Li-ion batteries used in existing electric buses in London city. The results demonstrate that the proposed Li-S battery pack can fulfil the requirements of an electric city bus in terms of power while achieving a considerable increase in vehicle's range with same weight of battery pack. However, Li-S cell prototypes still suffer from limited cycling life that prevents this technology to be commercialized for such an application at the time being.
Keywords— lithium-sulfur cell; modelling; battery pack sizing; simulation; electric bus

Published by Inderscience. This is the Author Accepted Manuscript issued with: Creative Commons Attribution Non-Commercial License (CC:BY:NC 4.0).
The final published version (version of record) is available online at DOI:10.1504/IJPT.2020.111227. Please refer to any applicable publisher terms of use.

Biographical notes:

Victor Calvo Serra is an automotive engineer specialised into electric and hybrid powertrains for automotive and motorsport applications. He obtained his MSc in Automotive Mechatronics at Cranfield University in 2018. He also acquired a Bachelor´s and Master´s degree in Industrial Engineering awarded by the Universitat Politècnica de Catalunya (Spain). He has developed a series of research projects related to electrification and hybridisation of vehicles, such as the design and simulation of battery packages for different applications. Furthermore, he has acquired hands-on experience taking part in Formula Student competition with the team ETSEIB Motorsport. Moreover, he led a group project at Cranfield University the objective of which was the design, development and demonstration of a parking technology solution for autonomous vehicles. Currently, he is working as an engineer at the company Integral Powertrain, which designs high power density electric motors and inverters for automotive and motorsport clients.

Abbas Fotouhi is a lecturer (assistant professor) in the Advanced Vehicle Engineering Centre at Cranfield University. Dr Fotouhi has more than ten years research experience in modelling and simulation, system identification, control system design and optimisation. Artificial intelligence (AI) and Machine Learning (ML) with applications in engineering problems is also part of his background. Before joining Cranfield, he was with the Centre for Artificial Intelligence and Robotics (CAIRO) at University Technology Malaysia. His current research is more focused on battery state estimation and also Intelligent Transportation Systems. Dr Fotouhi is an active member of the board who conduct MSc courses in Automotive and Motorsport Mechatronics at Cranfield University. His total writing portfolio lists over 40 articles and book chapters. He is an editorial board member of Neural Computing and Applications Journal, editorial board member of the Journal of Smart Science, and associate editor of International Journal of Strategic Engineering. He is a member of the Institute of Electrical and Electronics Engineers and fellow of the UK Higher Education Academy.

Mehdi Soleymani received his BSc, MSc, and PhD degrees from Iran University of Science and Technology (IUST) in 2000, 2003, and 2009 respectively. He is currently an associate professor of mechanical engineering at Arak University. Since August 2018 he is on detachment from Arak University and is with the Advanced Vehicle Engineering Centre (AVEC) at Cranfield University as a research fellow. His current research interest includes energy storage and energy management systems for hybrid electric, fuel cell, and electric vehicles.

Daniel J. Auger was born in Rainham, Kent, UK. He studied at the University of Cambridge receiving the BA/MEng degrees in electrical and information science in 2000, and the PhD degree in control engineering in 2005. From 2004 to 2008, he was a senior engineer with

BAE Systems, Chelmsford, UK. From 2008 to 2013, he was a senior consultant with MathWorks, Cambridge, UK. In 2013, he joined Cranfield University, Beds., UK, where he is currently a senior lecturer. His research is concerned with applications of control to electrified and automated vehicles, and he has established a successful research team developing BMS technologies for lithium-sulfur traction batteries. Dr Auger is a Chartered Engineer, a Fellow of the Institution of Engineering and Technology, and a Senior Member of the Institute of Electrical and Electronics Engineers. From 2013 to 2016, he was chair of the IEEE UK & Ireland Control Systems Society Chapter.

Nomenclature

A_f	Vehicle frontal equivalent area	N_s	Number of series cells
a	Vehicle acceleration	N_p	Number of parallel cells
C_D	Aerodynamic drag coefficient	P_{r_max}	Maximum required power
C_P	Battery/Cell polarization capacitance	P_T	Vehicle tractive power
E_{batt}	Battery pack energy	R_W	Vehicle wheel radius
F_D	Aerodynamic drag force	R_O	Battery/Cell ohmic resistance
F_{RR}	Road friction force	R_P	Battery/Cell polarization resistance
$F_{R\,TOT}$	Road total resistance force	SOC	State of charge
F_θ	Road grade force	$v_{vehicle}$	Vehicle speed
F_T	Vehicle tractive force	$v_{vehicle,max}$	Vehicle maximum speed
f	Rolling friction coefficient	V_{OC}	Battery/Cell open circuit voltage
G_{PID}	Driver model transfer function	V_{n_cell}	Nominal voltage of cell
I_{dmax_cell}	Maximum discharge current of cell	V_P	Battery/Cell polarization voltage
I_L	Batter/Cell load current	V_t	Battery/Cell terminal voltage
K_D	Differential control gain	v_{wind}	Wind speed
K_I	Integral control gain	η_T	Transmission system efficiency
K_P	Proportional control gain	θ	Road grade
m	Vehicle mass	δ	Equivalent inertia coefficient
$n_{motor,max}$	Electric motor maximum speed	ρ	Air density

1 - Introduction

Vehicle electrification technologies have been intensively considered in automotive industry in the past decades. Apart from the development needed in electric vehicle (EV) charging infrastructures, most of the challenges in development of EVs are currently related to the battery technology. High cost of batteries (Ehsani et al., 2018) which is expected to decrease in mass production in the coming years (Nykvist and Nilsson, 2015) is an example of such challenges. Other concerns regarding existing battery technologies, are vehicle range per one time battery charging, batteries' lifetime, charging time, battery safety, and operational temperature (Fotouhi et al., 2016b).

Electrochemical batteries are currently the most advanced energy storage technology in the EV market (Tie and Tan, 2013; Budde-Meiwes et al., 2013). Among different types of battery, Lithium-ion (Li-ion) is the dominant technology due to its desirable characteristics such as high energy and power densities, lack of memory effect, and low self-discharge (Budde-Meiwes et al., 2013). Depending on their constituent materials, Li-ion batteries fall into various categories with different performance characteristics (Fotouhi et al., 2016b; Battery University 2017). Although Li-ion batteries offer good features for EV application (Itani et al., 2017), their energy density is still limited to 200-250 Wh/kg (Fotouhi et al., 2016b). Figure 1 compares the energy density per mass and volumetric energy density of the Lithium battery with those of other available battery technologies.

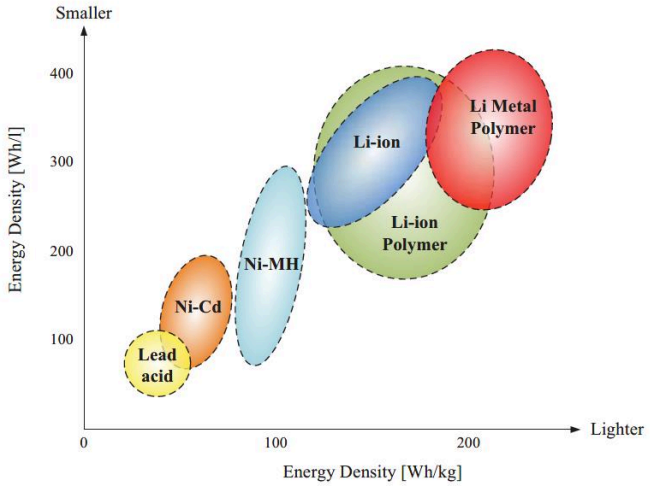

Figure 1: Energy density of various battery technologies (Stan et al., 2014)

To tackle this problem, other battery technologies are also under development such as lithium-air (Budde-Meiwes et al., 2013) and Lithium-Sulfur (Li-S). Li-S battery technology is promising mainly because of its superior energy density which can theoretically reach up to 500-600 Wh/kg (Budde-Meiwes et al., 2013; Wild et al., 2015). Furthermore, the price of Li-S cell, due to availability of sulfur and its low cost, would be potentially lower than that of Li-ion in mass production. Currently, Li-S cell prototypes have reached a specific energy of 400 Wh/kg (Wild at al., 2015) and volumetric energy density of 400-500 Wh/l (OXIS Energy, 2019: https://oxisenergy.com/technology/). However, self-discharge and low cycle life are still two undesirable features of this battery technology which arise as a result of capacity fade and cell degradation (Wild at al., 2015).

Useful reviews on Li-S cells technology readiness and their applications are discussed by Fotouhi at al. (2016b and 2017a) and Chen and Shaw (2014). The literature can be considered as two main areas: (i) studies that are focused on Li-S cell material development (Hagen et al., 2014; Li et al., 2016; Piwko et al., 2017) and electrochemical modelling (Hofmann et al., 2014; Ghaznavi and Chen, 2014) and (ii) researches in which the applications of Li-S battery technology are investigated (Propp et al., 2016 and 2017; Fotouhi et al., 2017b,c). Li-S battery has unique features (positive and negative) that need to be addressed in further studies. For example, one of the issues in the Li-S cell material optimization is related to the complex electrochemical reactions related to the conversion of elemental sulfur (S_8) to the final reduction product that is lithium sulfide (Li_2S) as explained in (Wild et al., 2015; Walus et al., 2013). The charging reactions have also same level of complexity where Li_2S_2 and Li_2S are converted to elemental sulfur (Walus et al., 2015) at the end. On the other hand, Li-S cell is not easy to handle for battery management system (BMS) because its states are not observable (due to the flat voltage curve) in a wide range of state-of-charge (SOC) as investigated by Fotouhi et al. (2017c). However, the first versions of Li-S cell SOC estimators are now available in the literature (Propp et al., 2017; Fotouhi et al., 2017c).

Looking at the literature, most of the researches around Li-S are focused on material development and electrochemical modelling of the cell rather than the application side. There is a research gap in the literature around investigation of Li-S cell's performance under real working conditions. Such studies can help electrochemist to develop more suitable cells which are tailored for each application. In this study, application of a new prototype Li-S cell in an electric city bus is studied. For this purpose, an electric bus with similar characteristics to an existing London city bus is

modelled and simulated under realistic driving conditions. Special attention is paid to the energy storage system used in the existing buses (i.e. Li-ion battery pack) and investigation of replacing them with a Li-S battery pack. For this purpose, design and sizing of the Li-S battery pack is performed based on the maximum power demand and the desired stored energy (desired range). As part of the EV modelling, a Li-S cell model is developed based on experimental laboratory tests as presented in Section 3. The cell model is then used to size the battery pack in Section 4.

2 - Vehicle Model

In order to evaluate performance of a Li-S cell under real working condition in an electric city bus, a vehicle simulation model is developed in this study. Three existing single decker London electric bus models including Irizar I2e (Irizar 2015), BYD 10.8M (BYD Europe 2015), and Optare Metrocity Bus (Optare Group 2017) have been considered. Due to the restrictions of having access to the full set of data of the commercial electric buses from the manufacturers, a generic vehicle model has been developed with similar features to current London electric buses (Gerald, 2016). The proposed model is built mainly based on the Irizar electric bus with specifications presented in Table 1.

Table 1: Electric urban bus model parameters

Model Parameter	Parameter Value	Model Parameter	Parameter Value
Air Density (ρ)	1.23 kg/m3	Aerodynamic Drag coefficient (C_D)	0.68 (Gowtham et al., 2016)
Frontal Equivalent Area (A_f)	7.6 m2	Wind speed (v_{wind})	0 m/s
Rolling Friction Coefficient (f)	0.007 (European Tyre & Rubber Manufacturers' Association, 2012)	Vehicle mass without battery (m)	13,000 kg
Equivalent Inertia Coefficient (δ)	1.075	Transmission Efficiency (η_T)	0.97 (BOSCH. 2014)
Vehicle Length	10,800 mm	Vehicle Width	2,500 mm
Vehicle Height	3200 mm	Vehicle Wheelbase	4,645 mm
Vehicle Weight Distribution (Front/Rear)	36.6% / 63.4% (Schoemaker, 2007)	Wheel Diameter (275/70 R22.5)	944 mm
Wheels Front Axle	2	Wheels Rear Axle	4
Road Gradient (θ)	0		

MATLAB/Simulink software is employed to model the vehicle's powertrain system that is a two-axle electric bus. Figure 2 illustrates schematic of the simulation model including battery, electric motor and a constant-ratio gearbox. The model's inputs are throttle and brake pedal signals (from the driver model) and the model's output is vehicle's speed. More details of the proposed model are explained in the following sections.

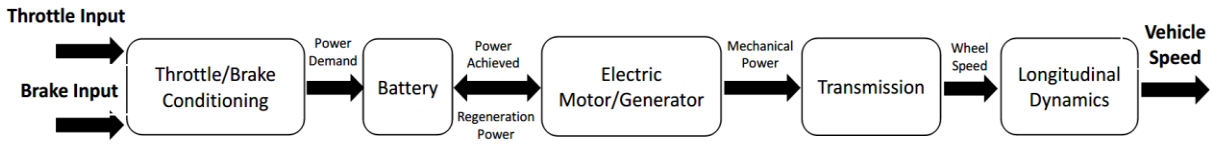

Figure 2: Electric bus simulation model's components

2.1 Driving Cycle and Driver Model

In order to simulate performance of the electric bus model with Li-S battery pack under real traffic conditions, the concept of driving cycle has been employed. The Millbrook London Transport Bus (MLTB) cycle (Barlow et al., 2009; Low Carbon Vehicle Partnership, 2018) is used in this study because it represents the driving conditions in central London quite well. In the simulations, MLTB cycle is used as the reference velocity profile. Furthermore, a driver model is designed to achieve the desired speed profile during the simulations. The driver model is a closed-loop proportional Integral Differential (PID) controller that works based on the error between the reference velocity and the vehicle's velocity as shown in Figure 3. The PID controller has the following transfer function:

$$G_{PID}(s) = K_P + \frac{K_I}{s} + K_D s \quad (1)$$

where K_P, K_I and K_D are controller's gains which are tuned in a way to fulfil both maximum overshoot and settling time criteria. Figure 4 illustrates the controller's performance in response to a step velocity input. As shown in the figure, the maximum 5% overshoot has been achieved within around 1 second that is an acceptable settling time for this application since the drive cycle frequency is 1 Hz. The controller's gain values are presented in Table 2. Figure 5 compares the reference and achieved velocity profiles using the proposed driver model over MLTB driving cycle simulation case study. As shown in the figure, the driver model is able to effectively follow the reference speed profile (i.e. drive cycle).

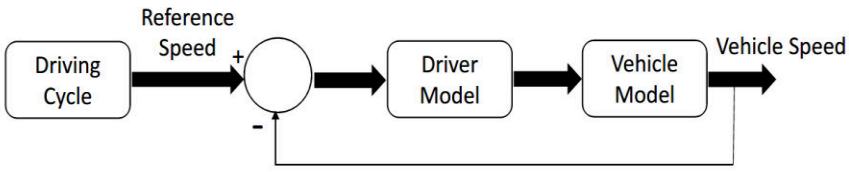

Figure 3 : Reference velocity tracking using PID controller

Table 2: Driver PID model's parameters

PID gain	Value
K_p	30
K_I	65
K_D	0

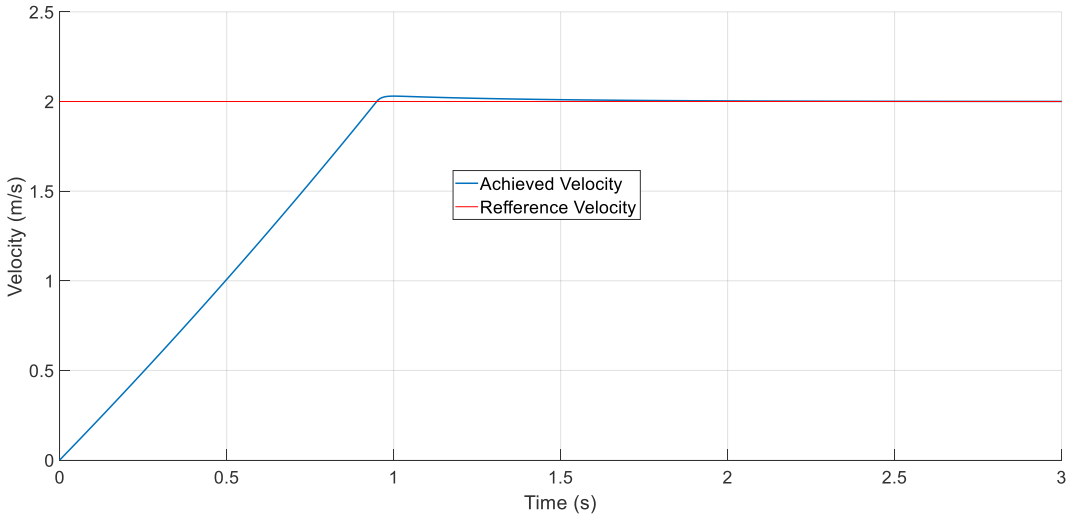

Figure 4: Step response of the driver model

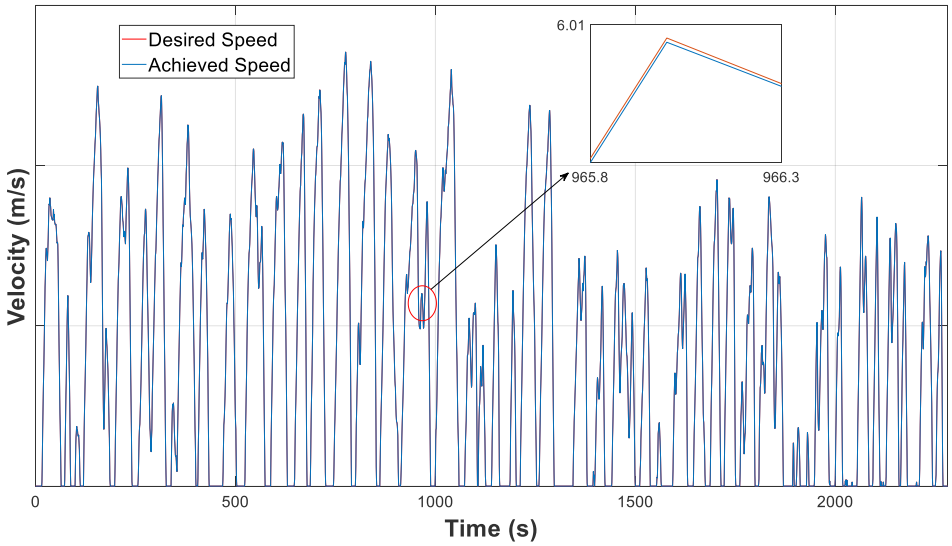

Figure 5: Desired and achieved speeds comparison at MLTB driving cycle

2.2 Vehicle's Longitudinal Dynamics

Vehicle's longitudinal dynamics is modelled by considering the following resistance forces presented in equations (2)-(5), where equation (2) describes the aerodynamic drag force and equations (3) and (4) show the friction and road grade forces respectively. The parameter, $V_{vehicle}$, is the vehicle's speed and the other parameters are as previously introduced in Table 1. The road total resistance force is then given by equation (5).

$$F_D = \frac{1}{2}\rho C_D A_f (v_{vehicle} + v_{wind})^2 \quad (2)$$

$$F_{RR} = f m g \cos(\theta) \quad (3)$$

$$F_\theta = m g \sin(\theta) \quad (4)$$

$$F_{R\,TOT} = F_D + F_{RR} + F_\theta \quad (5)$$

Considering the vehicle's tractive force (F_T) and the road total resistant force, vehicle's acceleration is calculated as follows:

$$F_T - F_{R\,TOT} = (m + m_e)a = \delta m a \;\; ; \;\; a = \frac{F_T - F_{R\,TOT}}{\delta m} \quad (6)$$

where m and m_e are vehicle mass and rotating inertia equivalent mass respectively. The vehicle's tractive force is also obtained using equations (7) and (8) in which P_T is the tractive power or the brake

regenerative power, η_T is the transmission system's efficiency, and $P_{EM/Gen}$ is the electric motor/Generator's output power.

$$F_T = \frac{P_T}{v_{vehicle}} \quad (7)$$

$$P_{T/Reg} = \eta_T . P_{EM/Gen} \quad (8)$$

2.3 Electric Motor and Transmission System

The transmission system provides a constant gear ratio between the electric motor and the driven axle. The gear ratio selection depends on the electric motor's specifications and the vehicle's speed range. The electric motor that is used in this application is REMY's HVH410-150-DOM, offered by the company REMY International which is acquired by BorgWarner company in 2015 (BorgWarner, 2016). Specifications of the motor are presented in Table 3 along with the motor efficiency map that is shown in Figure 6 and the torque-speed motor curve displayed in Figure 7. Since the electric bus is expected to be used in urban traffic condition, the maximum vehicle's required speed is assumed to be 98.6 km/h according to the MLTB driving cycle. Consequently, the transmission ratio is calculated to be 10.8 using Equation (9).

$$v_{vehicle,max}\left(\frac{m}{s}\right) = \frac{n_{motor,max} \cdot 2 \cdot \pi \cdot R_W}{60 \cdot i} \; ; \; i = \frac{n_{motor,max} \cdot 2 \cdot \pi \cdot R_W}{60 \cdot v_{vehicle,max}} \quad (9)$$

Table 3: Electric motor REMY HVH410-150-DOM main parameters (Remy International – BorgWarner, 2012)

Motor Parameter	Value	Motor Parameter	Value
Peak Power	295 kW	Peak Motor Torque	1,700 Nm
Motor Speed Range (n)	0-6,000 min^{-1}	DC Voltage Input Range	200-700 V
Motor Mass	148 kg	Motor Rotational Inertia	1.09 kgm^{-2}
Peak Motor Current	480 Arms	Transmission Gear Ratio (i)	10.8

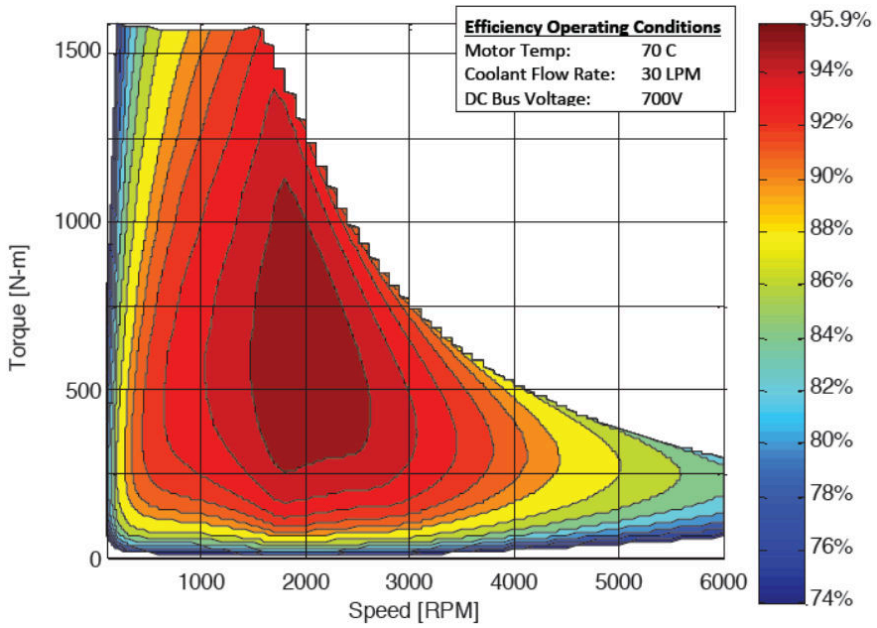

Figure 6: Electric motor REMY HVH410-150-DOM efficiency map (Remy International 2012)

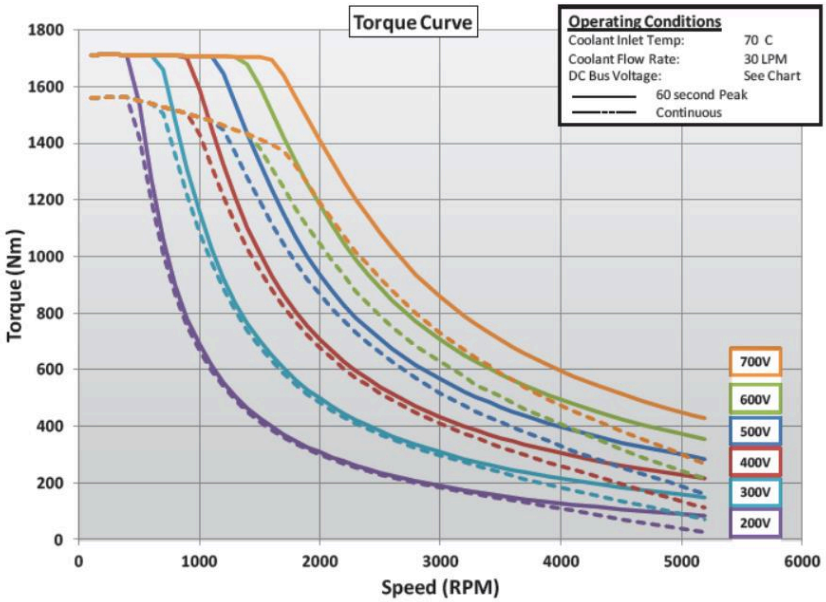

Figure 7: Electric motor REMY HVH410-150-DOM motor torque and speed curves (Remy International 2012)

Regenerative braking strategy is a serial type with the blending control scheme as presented in (Chen, 2018). According to this braking strategy, for low torque demands, the braking torque is entirely provided by the electric motor (generator) and the regenerated energy is limited by the

battery maximum charge current. For higher torque demands, the friction brake is also activated in conjunction with the regenerative brake system (Chen, 2018; Varocky, 2011).

3 - Li-S Cell Modelling

As mentioned before, feasibility of employing a new Li-S prototype cell in an electric bus is investigated in this study. Specifications of the prototype cell, provided by OXIS Energy (2018), is presented in Table 4. For Li-S cell model parameterization, a formal 'system identification' technique is used including three main parts: 1) model structure selection, 2) experimental test, and 3) Fitting the model into test data.

An equivalent circuit network (ECN) model, called Thevenin model, is employed as the model structure shown in Figure 8. ECN modelling technique is a common approach to simulate cell's performance in the literature. With less complexity comparing to electrochemical models, ECN cell models have been used in a wide range of applications (Fotouhi et al., 2016a). In the model shown in Figure 8, V_t is terminal voltage, V_{OC} is open circuit voltage, R_O is ohmic resistance, R_P and C_P are equivalent polarization resistance and capacitance respectively. Differential equations of such a model are presented in equation (10):

$$\begin{cases} V_t = V_{OC} - R_O.I_L - V_P \\ \dfrac{dV_P}{dt} = -\dfrac{1}{R_P C_P} V_P + \dfrac{1}{C_P} I_L \end{cases} \quad (10)$$

Table 4: Specifications of prototype Li-S pouch cell

Parameter	Value
Capacity	19 (Ah)
Nominal voltage	2.15 (V)
Cell mass	141 (g)
Maximum voltage	2.6 (V)
Minimum voltage	1.9 (V)
Maximum discharge rate	3C ~ 57 (A)
Maximum charge rate	0.25C ~ 4.75 (A)

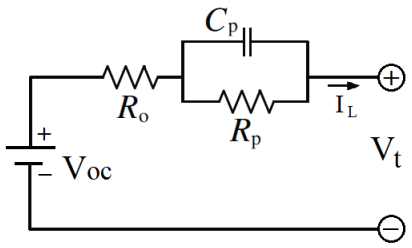

Figure 8: Equivalent circuit cell model (Thevenin model)

After choosing the model structure, the second part of the model identification process is experimental test design. The experimental test setup used in this study is shown in Figure 9 including: (i) a power source/sink that applies a desirable current profile to the cell and measures its terminal voltage, (ii) a thermal chamber to control the temperature during the test, and (iii) wiring and the cell's fixture that is an aluminium box.

Figure 10-(a) shows a mixed pulse discharge test which was used for Li-S cell model parameterization in this study. Pulse tests are common in the literature to be used for cell characterization. The pulse tests used in this study were designed based on the cell's specifications (i.e. maximum discharge current) and were intended to give data sets that allow the dynamics of interest to be clearly seen. The test process contains consecutive discharge pulses applied to the Li-S cell. Various discharge rates (i.e. 0.05C, 0.25C and 0.5C) are considered. Duration of each pulse is 30 seconds and there is 120 seconds relaxation between each two consecutive pulses. The test started at fully-charged state (2.6 V) and continued until the cell's terminal voltage dropped below the cut-off voltage (1.9 V) that means depleted state (0% SOC). Actually, this is an agreement to consider 0% SOC when the open circuit voltage reaches to a minimum value called 'cut-off voltage'. This number is determined by the cell manufacturer to avoid cell damage during discharging. In our test, because the discharge current is not high and we have considered enough relaxation between pulses, the assumption of 0% SOC when the voltage hits to the cut-off voltage can be true. However, it should be noted that there might still be a bit of energy inside the cell even after reaching to that limit.

In addition to the pulse test, MLTB test is also performed on a single cell by scaling the current demand to match to the single cell capabilities. Figure 10-(b) demonstrates current and terminal voltage of the cell during that test. The result is showing that the prototype cell is performing quite well under real operating condition too. In both tests, measurement data were collected at sampling

rate of 1 Hz. The measurements included time, current and the cell's terminal voltage while temperature was monitored to ensure that it is being kept constant at 20°C during the test.

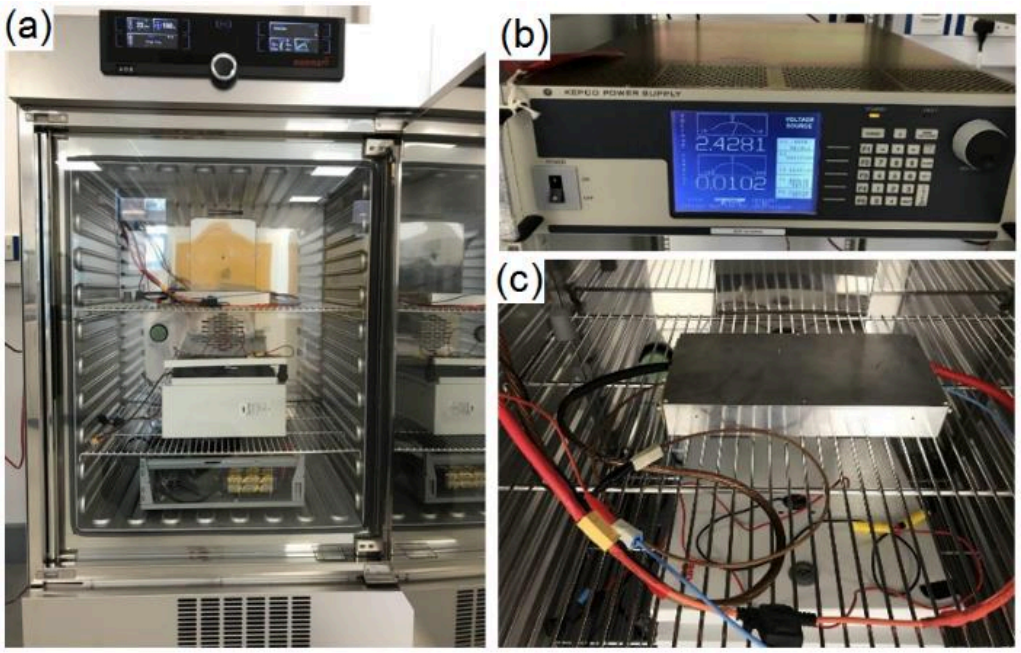

Figure 9 : Cell test equipment: (a) thermal chamber, (b) power source/sink, (c) Li-S cell inside an aluminium box

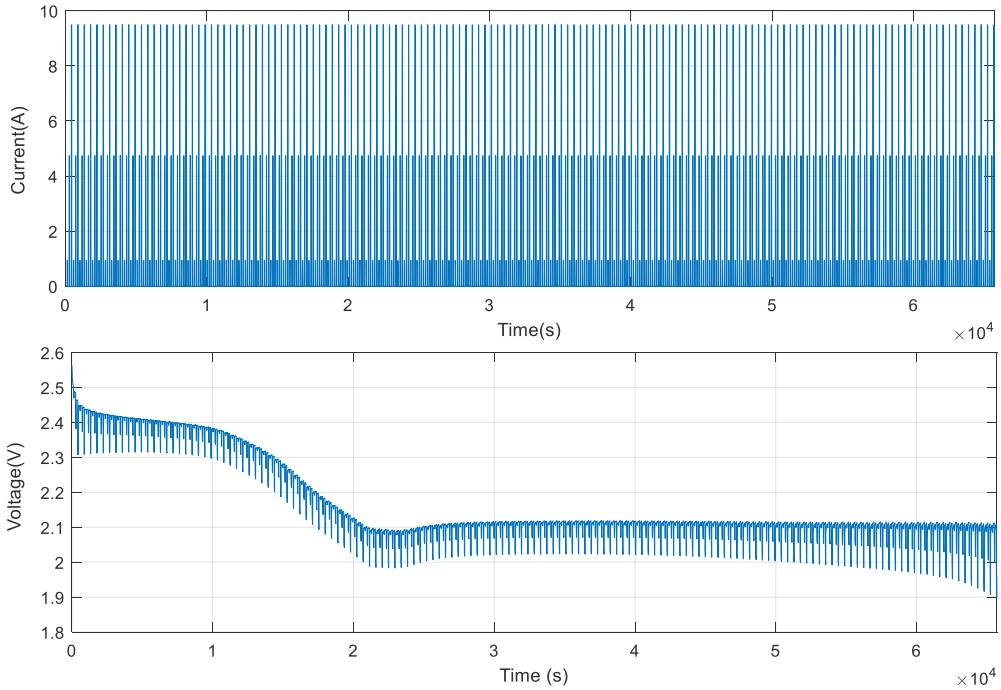

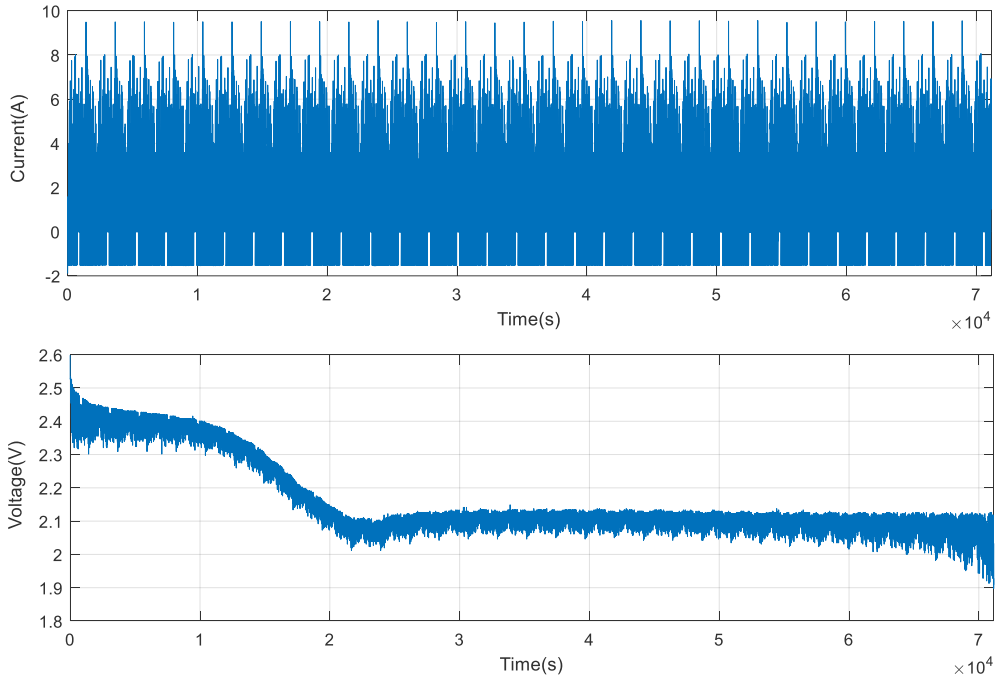

Figure 10 : Current profile and cell's terminal voltage during (a) mixed pulse discharge test, (b) MLTB test

After model structure selection and experimental test design, the third part of the system identification approach is to fit the model into the test data. For this purpose, the well-known Prediction-Error Minimization (PEM) algorithm is used for cell model parameterization. The identification algorithm minimizes the error between the ECN model's prediction and the measurement (experimental data). For this specific application where the cell's parameters are changing slowly with regard to SOC, the PEM algorithm is fast enough to identify this time-varying model as discussed by Fotouhi et al. (2016a). Using the PEM algorithm and experimental data, the parameters of the Thevenin model are obtained for the new Li-S prototype cell as shown in Figure 11. The cell model's parameters are imported into MATLAB/Simulink simulation platform as look-up tables to build a battery model for vehicle simulation case-studies in the following section. In the simulation model, battery SOC is updated at each time step by using the coulomb-counting technique that is the integration of current over time.

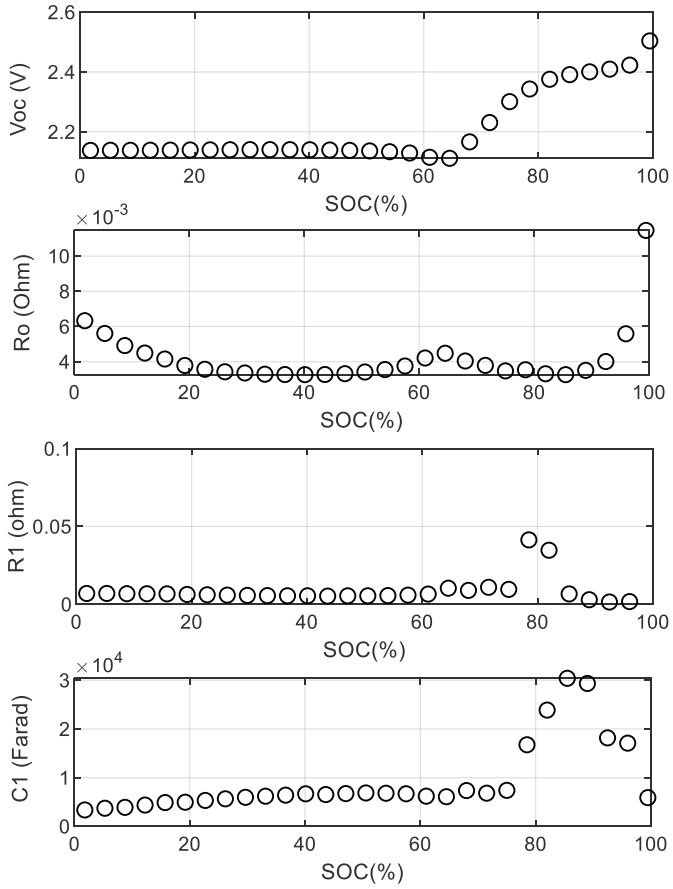

Figure 11: Equivalent Circuit Network Li-S model parameters

4 - Li-S Battery Pack Sizing and Performance Analysis

The cell model developed in previous section, is used here to develop a battery pack simulation model. A battery pack design process generally includes many different aspects such as designing the cooling system, BMS, structure of the pack, connectors and wiring, etc. Here, the whole process of battery pack design is not covered since it contains lots of discussions that are out of the framework of this study. This work is only focused on battery pack sizing which means determination of number of cells and their configuration in series or parallel connections. There are assumptions used in the proposed battery pack model such as: (i) all cells are assumed to be identical and they are fresh cells without any degradation, (ii) the effect of temperature gradient inside the pack is neglected and all cells are assumed to work at a constant temperature controlled by the BMS, (iii) the internal resistance of the connectors and wirings inside the pack is not considered in the simulations. Using these assumptions, performance of the battery pack is quite

similar to the individual cell but in a larger scale. This is an 'ideal' scenario however, the authors believe that those assumptions don't affect the overall conclusion of this study.

Two separate approaches have been employed for sizing of the Li-S battery pack in electric bus application. In the first approach, called 'power-based sizing', the battery pack size is determined based on the maximum required power to run the EV over MLTB cycle. This approach is explained in Section 4.1. In the second approach, called 'energy-based sizing', the battery pack size is calculated based on the maximum stored energy in the battery that directly determines the range of EV. In order to size the Li-S pack in this approach, the range of a couple of existing operational electric buses in London city is considered as benchmark. The second approach is explained in Section 4.2.

4.1 Power-based battery pack sizing

The reason for sizing based on power is to ensure achievement of the required maximum power with minimum number of battery cells. At the same time, estimation of the vehicle range based on this approach is the second goal. In order to size the Li-S battery pack based on the maximum required power, called 'power-based sizing', EV model is simulated over the MLTB driving cycle. Such a simulation case-study would give us the power demand signal that is expected to be provided by the vehicle's powertrain system. The battery pack can then be sized properly to provide the required power by considering all the efficiencies, etc.

Although 140 kW seems to be sufficient for MLTB cycle, the real electric buses in the market are a bit more powerful than that. For example, the Irizar I2e electric bus (Irizar, 2015), that is operational in London city, has two 90 kW electric motors (180 kW in total). For this reason, the Li-S battery pack is also sized based on 180 kW to meet the requirements of the existing Li-ion battery packs used in the market.

In order to determine the number of cells in series, the battery voltage constraint is considered to be below 700 V according to the electric motor and converter safety instructions (Remy International – BorgWarner, 2012). Therefore, 269 Li-S cells are connected in series in the pack by assuming 2.6 V as the maximum cell's voltage. Having 269 cells in each circuit, the number of parallel circuits (N_p) is obtained as follows:

$$N_p = \frac{P_{r,max}}{N_s \ . \ V_{n,cell} \ . \ I_{dmax,cell}} \quad (11)$$

where $P_{r,max}$ is the maximum required power, N_s is the number of cells in series (i.e. 269), $V_{n,cell}$ is the single cell's nominal voltage and $I_{dmax,cell}$ is the single cell's maximum discharge current. Table 5 presents the power-based Li-S battery pack sizing results. The result is showing that 5 parallel circuits (i.e. 1345 cells in total) would be sufficient to provide the maximum power of 180 kW in an electric city bus. Figure 13 illustrates the proposed battery pack's SOC, current and terminal voltage over repeating MLTB simulation case-study. The simulation is started from fully charged state (SOC=100%) and it is continued until depleting the battery (zero SOC). There are two different regions (plateaus) in Li-S voltage curve which are caused by different electrochemical reactions taking place inside the cells: (i) high plateau from 100% charge to approximately 70% (can change depending on temperature and discharge rate), and (ii) low plateau starting from the break point around 70% until zero SOC. The Li-S battery pack's voltage is quite stable over the low plateau region which is a good feature in terms of easier matching of the other components such as power electronics and electric motor. More discussions around the reasons of this unique behaviour of the Li-S cell can be found in (Wild et al., 2015).

Table 5. Power-based Li-S battery pack sizing results

Parameter	Value	Parameter	Value
Number of cells in series	269	Nominal Voltage	578 V
Number of parallel circuits	5	Maximum Discharge Current	285 A
Battery pack's energy	55 kWh	Maximum Charge Current	24 A
Cells' total mass in the pack	190 kg		

Figure 12 demonstrates battery power demand in the electric bus model that is simulated over MLTB driving cycle. As shown in the figure, the maximum required power in such a driving scenario is under 140 kW which is well below the maximum power of the electric motor. On the other hand, the negative power (that is limited to 14 kW) is due to energy regeneration during braking. The limitation of negative power is due to battery capability to accept high charge current

as mentioned in Table 4 (for a single cell) and by considering the battery configuration (269 cells in series and 5 parallel strings).

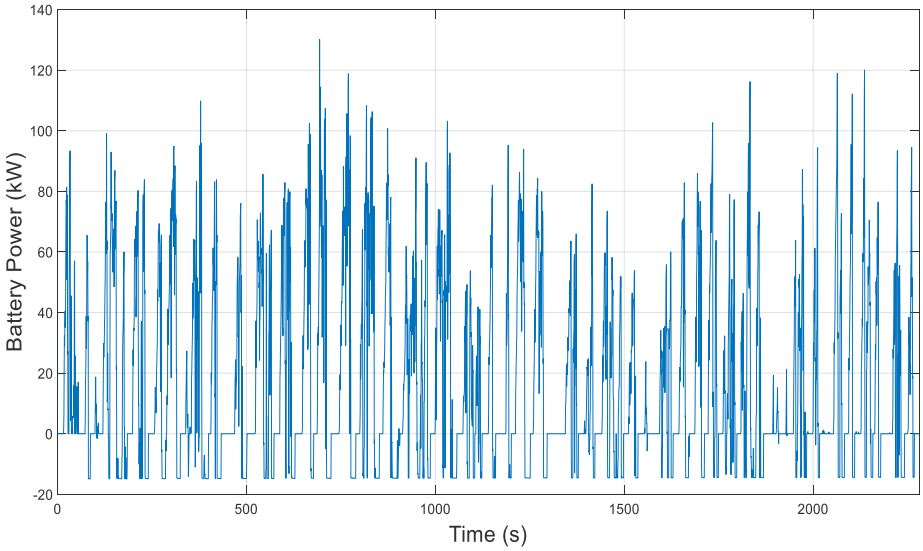

Figure 12: Battery power demand in electric bus model over MLTB driving cycle

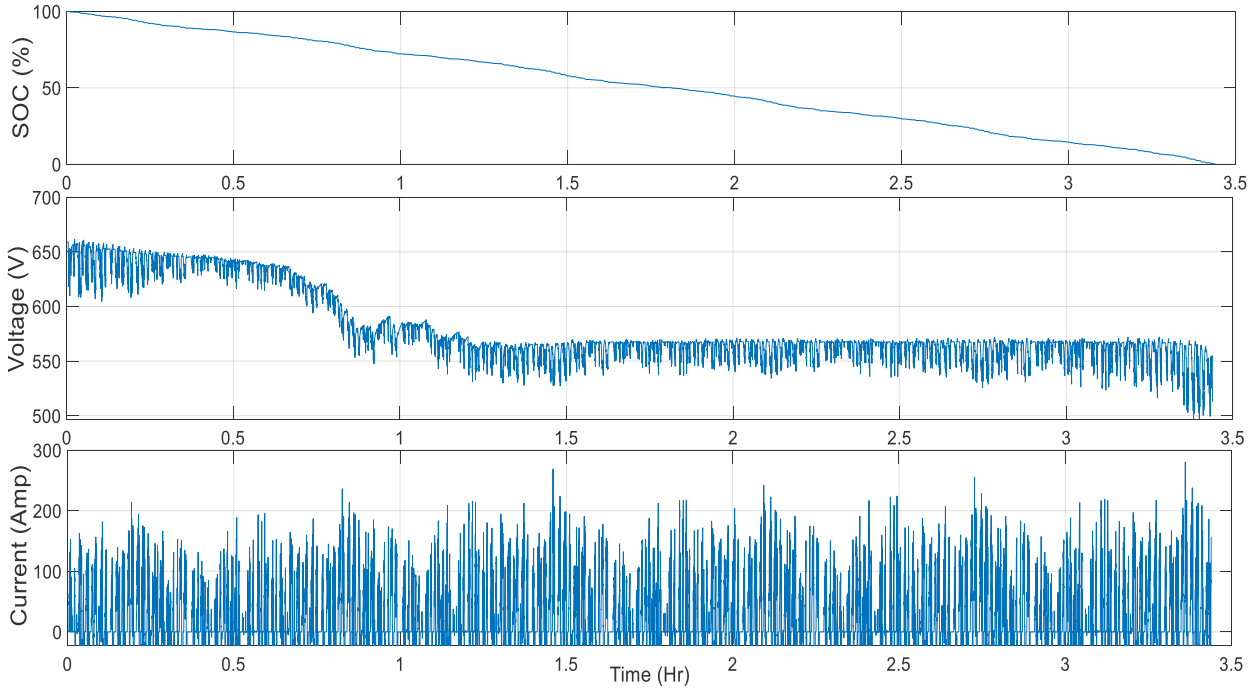

Figure 13: Battery pack response variables after sizing based on the electric power demand

4.2 Energy-based battery pack sizing

In the second sizing approach, called energy-based sizing, the Li-S battery pack is expected to have a certain amount of energy in kWh. According to the specifications of the Irizar electric bus (Irizar, 2015), the Li-ion battery pack that is used in that vehicle has 282 kWh energy on board when it is fully charged. Assuming that the proposed Li-S battery pack should also have same amount of energy to guarantee attaining the desired range, the number of parallel circuits (N_p) is calculated using equation (12).

$$N_p = \frac{E_{batt}}{N_s \,.\, V_{n,cell} \,.\, C_{cell}} \qquad (12)$$

where E_{batt} is the expected total energy (Wh) of the battery pack, N_s is the number of cells in series (calculated as explained in Section 4.1), C_{cell} is the capacity of each cell in Ah, and $V_{n,cell}$ is the nominal voltage of a single cell. Table 6 contains the battery pack sizing results based on the required stored energy criterion. The result is showing that 26 parallel circuits (i.e. 6994 cells in total) would be sufficient to provide the required energy on board. An obvious outcome is that sizing the pack based on required energy also guarantees the maximum power demand discussed in Section 4.1. So in the following parts of this study, this energy-based sizing result is used. Figure 14 shows the proposed battery pack's SOC, current and terminal voltage under the repeating MLTB simulation case-study. The simulation is started from fully charged state (SOC=100%) and it is continued until depleting the battery (zero SOC).

Table 6. Energy-based Li-S battery pack sizing results based on expected stored energy

Parameter	Value	Parameter	Value
Number of cells in series	269	Nominal Voltage	578 V
Number of parallel circuits	26	Maximum Discharge Current	1482 A
Battery pack's energy	286 kWh	Maximum Charge Current	124 A
Cells' total mass in the pack	986 kg		

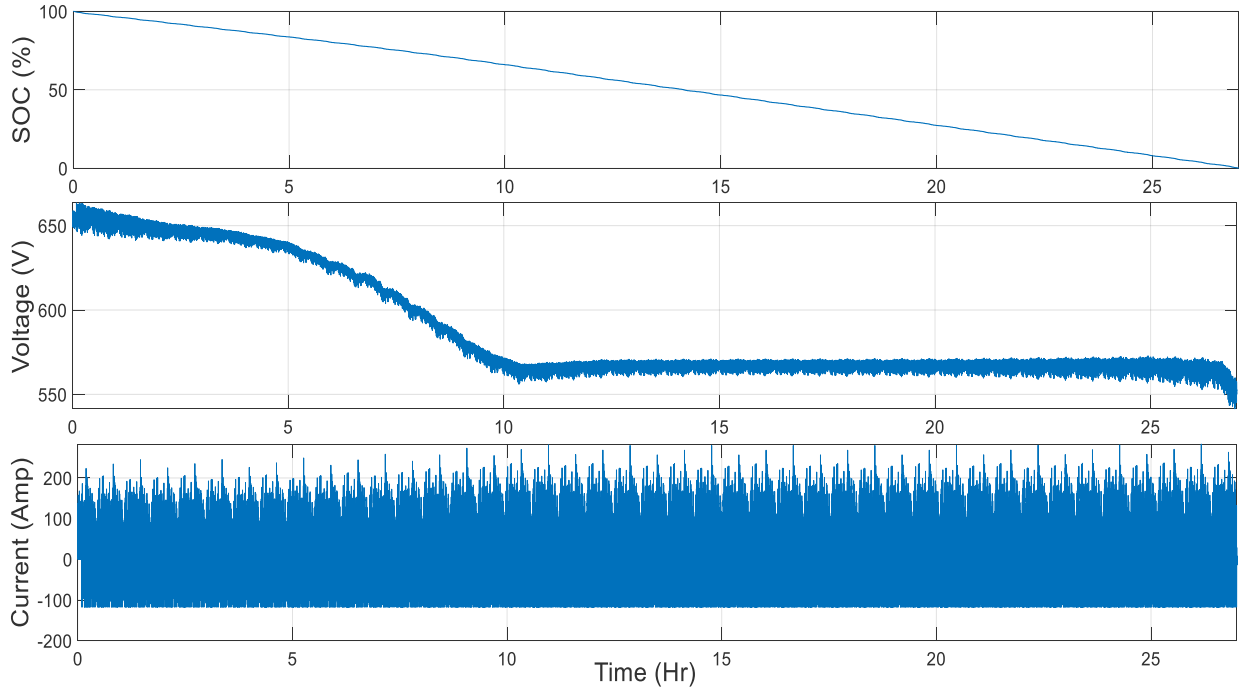

Figure 14: Battery response variables for the energy-based sizing

4.3 Comparative analysis

In Section 4.2, Li-S battery pack was sized to have same amount of energy comparing to an existing Li-ion battery pack used in an electric bus. The simulation results demonstrated that the proposed Li-S battery pack can provide sufficient power and energy for electric city bus application. Now the question is what are the advantages/disadvantages of this new technology comparing to the existing Li-ion technology? For this comparison, different features of the Li-S cell should be considered such as energy density, power density, cycle life, cost, safety, etc. However, a comprehensive investigation of all these features is out of the scope of this study. Our model-based analysis can help us to investigate energy and power but not the other features. Li-S cell's cycle life, cost and safety will be briefly mentioned later based on the literature.

Cell's energy density directly affects the total mass of the battery pack that is a key factor in EV design. It can affect not only the vehicle longitudinal dynamics and range, but also the vehicle's ride quality and stability (Crolla and Cao, 2012). In this study, impact of the battery pack's mass on EV range is investigated using the proposed simulation model. For this purpose, a sensitivity analysis is conducted and the vehicle's range is calculated as a function of the battery pack's mass. Two existing Li-ion battery types including Lithium Iron Phosphate (LiFePO4) and Lithium Nickel

Manganese Cobalt Oxide (LiNiMnCoO2 or NMC) have been considered as benchmarks to be compared with Li-S. The reason of choosing those Li-ion batteries is that both of them are currently used in electric buses in London city (BYD Europe, 2015; Optare Group Ltd., 2017). Specifications of these two Li-ion cells are presented in Table 7.

Table 7: Li-ion cells' specifications (AA Portable Power Corp, 2012)

Cell Feature	**Headway LiFePO4 10Ah Cell**	**AA Portable Power Corp $LiNiMnCoO_2$ 10Ah Cell**
Nominal Voltage	3.2 V	3.7 V
Minimum / Maximum Voltage	2.0 V / 3.6 V	2.75 V / 4.2 V
Capacity	10 Ah	10 Ah
Geometry	38 mm (diameter), 132 mm (length)	170 x 60 x 11 mm (length x width x thickness)
Mass	330 g	200 g
Energy Density	105 Wh/kg	185 Wh/kg
Maximum Discharge Current	100 A (Peak 150 A)	100 A
Maximum Charge Current	30 A	10 A
Cycle Life	1500 cycles	500 cycles

Figure 15 illustrates sensitivity of the electric bus range to battery pack's mass over repeating MLTB cycle. In this comparative study, all battery packs have same amount of energy (kWh) but they are different in weight due to the difference in cell's energy densities. The weight of BMS components, connectors and wirings, battery pack's case, etc., is also considered by multiplying a modification factor of 1.75 to convert cells' weight to battery pack's weight. It should be noted that this modification factor can change from a pack manufacturer to another, or from cell to cell. For example, a bit higher value is reported for Nissan LEAF (Qnovo, 2015). In this study, we have considered a fixed number for fair comparison. According to Figure 15, the vehicle's range has increased 8% and 21% using Li-S battery pack in comparison with $LiNiMnCoO_2$ and $LiFeO_4$ batteries respectively. This range augmentation has been achieved just as a result of the vehicle's mass reduction due to the battery pack lightweighting.

In another analysis, the vehicle's range is investigated when the Li-ion battery pack is replaced by a same-weight Li-S battery pack. In this analysis, Li-S battery pack is sized to have the same weight

as $LiNiMnCoO_2$ and $LiFeO_4$ battery packs. This means that we can now have a bigger Li-S battery pack comparing to the previous analysis where the energy (kWh) of the packs were same. Same-weight battery pack sizing is a correct assumption when there is no volume limitation. This is not definitely possible in a compact car however, might be possible in an electric bus or truck where we have more space. Figure 16 compares the vehicle's range using three different battery packs: (*i*) original Li-S pack that guarantees the minimum range by providing 286 kWh energy as explained in Section 4.2, (*ii*) a modified Li-S pack that is sized to have same weight as the existing $LiNiMnCoO_2$ battery pack, and (*iii*) a modified Li-S pack that is sized to have same weight as the existing $LiFeO_4$ battery pack. As shown in the figure, the vehicle's range increases drastically when the Li-ion battery packs are replaced by their mass-equivalent Li-S packs.

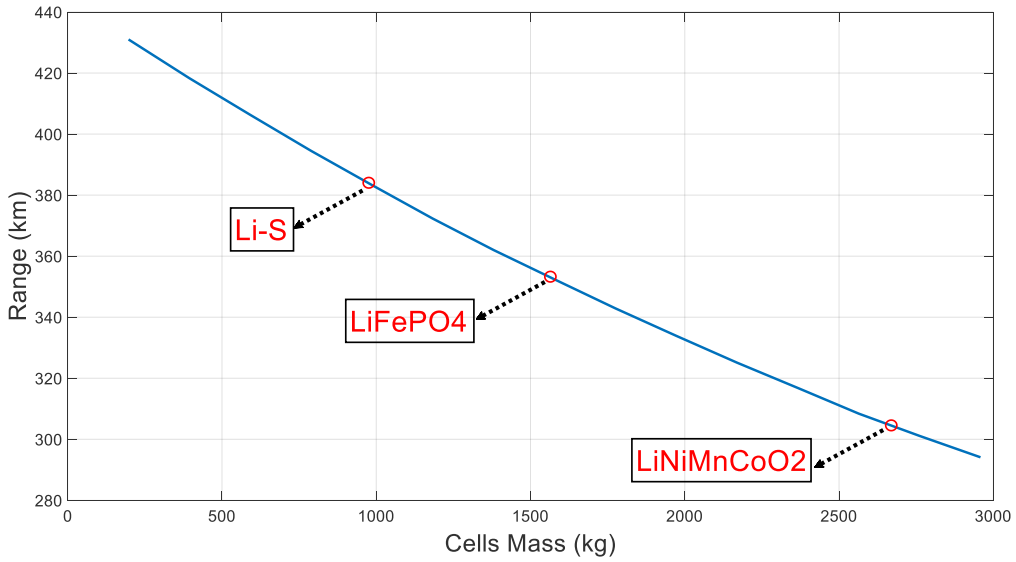

Figure 15: Sensitivity of the electric bus range to battery pack's mass over repeating MLTB cycle – all battery packs have same amount of energy (kWh) but they are different in weight

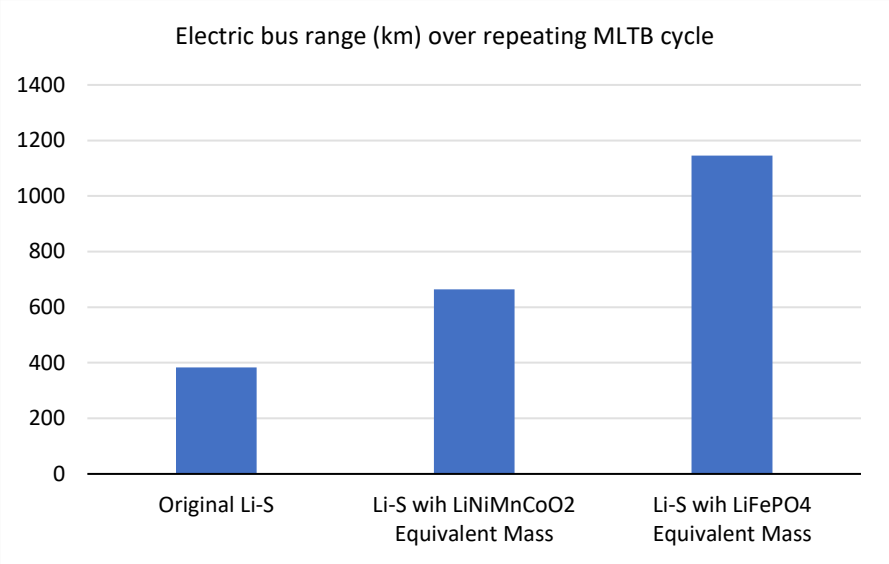

Figure 16: Electric bus range over repeating MLTB cycle – all battery packs are built from Li-S cell but they are different in size and energy (kWh)

Although our model-based investigations demonstrate a significant improvement in vehicle's range when using Li-S technology in an electric city bus, other aspects of this technology should be also considered. Energy density, as one of the main advantages of Li-S battery technology, is quite promising. Battery lightweighting can bring lots of benefit in energy conservation. On the other hand, Li-S is not as good as Li-ion in terms of power density. As an example for comparison, power density of the carbon coated LiFePO4 (C-LFP) is around 3.3 kW/kg at 30°C (Hwang et al. 2017) whereas it is around 800 W/kg for the Li-S prototype cell that is used in this study. However, our simulation results demonstrate that providing the maximum power demand in an electric city bus application wouldn't be an issue for the Li-S battery pack. In terms of the cost, an exact number is not available since the existing Li-S cells are all hand-made prototypes however, Li-S cell's price is expected to be less than the existing Li-ion cells in mass production due to availability of sulfur (Fotouhi et al., 2017a; Hagen et al., 2015; Hunt et al., 2015). Safety is also an advantage of Li-S battery technology in comparison to other competitors (Hagen et al., 2015; Hunt et al., 2015). On the other hand, one of the disadvantages of Li-S cell is its limited charging rate in comparison with Li-ion technologies in the market. This can affect the charging time and also regenerative braking. However, this limitation is more important for constant charging rather than instantaneous charge pulse due to regenerative braking (0.25C charge rate is currently suggested by the cell manufacturer for constant charging but the limit is higher for short-time pulses). Slow EV overnight charging is

the best way of charging even for Li-ion batteries by considering the cell degradation. Li-S would be more sensitive to the charging pattern and the existing prototype cells can only accept this type of charging. It should be also noted that the cells are under development and better specifications are expected in the next generation of cells. Another main disadvantage of Li-S cell is its limited cycle life in comparison to Li-ion cells. At the time being, Li-S prototype cells can reach to hundreds of cycles whereas for Li-ion cells, this number is around 1000 to 2000 cycles (this number is less for LiMn2O4). This might be manageable for space applications where the weight is quite critical and less cycle life is needed. However, for automotive application, Li-S cells are still far from the market's requirements mainly because of the limited cycle life.

5 - Conclusions

In this study, suitability of a new Li-S cell for electric city bus application was investigated. A vehicle powertrain system model was developed based on the specifications of existing electric buses in London city. In order to build a Li-S battery pack model, experimental tests were conducted on a single cell and an ECN cell model was parameterized. The Li-S battery pack was then sized for the electric city bus application based on the single Li-S cell's characteristics and also powertrain system's requirements. Two approaches were employed for battery pack sizing based on the maximum required power and required energy (range) on MLTB driving cycle. Simulation results demonstrated that the proposed Li-S battery pack can fulfil both the power and energy requirements in an electric city bus. Furthermore, performance of the proposed electric bus model that was equipped with Li-S battery was compared with two existing electric buses with $LiNiCoO_2$ and $LiFeO_4$ battery packs. According to the results, the vehicle's range has increased 8% and 21% using Li-S battery pack in comparison with $LiNiCoO_2$ and $LiFeO_4$ batteries respectively just as a result of battery pack lightweighting. In our second analysis, modified Li-S packs were sized to have same weight as the existing Li-ion battery packs. Those results demonstrated that the vehicle's range increases drastically when the Li-ion battery packs are replaced by their mass-equivalent Li-S packs due to the high energy density of Li-S battery. On the other hand, power density of Li-S is not as good as that for Li-ion. However, our results showed that this limitation wouldn't cause any issue in this particular application (i.e. electric city bus). Regarding the other features of Li-S cell such as cost, safety and cycle life, the last one seems to be the bottleneck at the time being. The existing Li-S prototype cells can reach to hundreds of

cycles whereas for Li-ion cells, the cycle number is higher. This might be manageable for space applications where the weight is quite critical and less cycle life is needed. However, for automotive application, Li-S cells are still far from the market's requirements mainly because of the limited cycle life.

This paper had some novelties that we believe they can contribute to the existing literature. The first novelty is about the stat-of-the-art Li-S cell that was used here. It is one of the latest versions of Li-S cell that was received from one of the largest Li-S cell manufacturers in the world. So, the results of this study can contribute to the literature by providing new test results. The second main contribution of this study is the application that is an electric city bus. Such an application doesn't exist in the literature. We believe it would be useful for researches in this area to see how such a new technology behaves under real driving condition; for example, how many of these cells are necessary for that application, etc. We appreciate all the existing materials available in the literature and we hope this study can contribute to those by presenting new results and outcomes. Of course, this study will not be the last one in this area and more research studies are needed until making Li-S technology ready for the market. It should also be mentioned that different Li-S cell prototypes are under development and it is a promising technology with remarkable progress during last decade.

References

AA Portable Power Corp (2012) "LiNiMnCoO2 High Power Cell 3.7 V 10 Ah Lithium-Ion Battery," 10059156-5C, Richmond, CA.

Barlow T. J., Latham S., McCrae I. S., Boulter P. G. (2009) "A reference book of driving cycles for use in the measurement of road vehicle emissions, Wokingham: TRL Ltd.

Battery University (2017) "Types of Lithium-Ion," 15 11 2017. [Online]. Available: http://batteryuniversity.com/learn/article/types_of_lithium_ion. [Accessed 20 06 2018].

BorgWarner (2015) "Borgwarner Enters into Agreement to acquire Remy International", 13 07 2015. [Online]. Available: https://www.borgwarner.com/news-media/press-releases/2016/08/19/borgwarner-enters-into-agreement-to-acquire-remy-international. [Accessed 2018 05 03].

BOSCH (2014) "Automotive Handbook", Germany: John Wiley & Sons Ltd.

Budde-Meiwes H., Drillkens J., Lunz B., Muennix J., Rothgang S., Kowal J. (2013) "A review of current automotive battery technology and future prospects," *Journal of Automobile Engineering,* no. 227(5), pp. 761-776.

BYD Europe (2015) "Pure Electric Buses Catalogue," Rotterdam.

Chen L., Shaw L.L. (2014) “Recent advances in lithium–sulfur batteries”, J. Power Sources, 267, 770–783.

Chen L. (2018) “Hybrid Braking of Electrified Vehicles: Design, Modelling and Control,” Advanced Vehicle Engineering Centre, Cranfield University, UK.

Crolla D. A., Cao D. (2012) “The impact of hybrid and electric powertrains on vehicle dynamics, control systems and energy regeneration”, Vehicle system dynamics, 50.sup1, 95-109.

Ehsani M., Gao Y., Longo S., Ebrahimi K. (2018) “Modern Electric, Hybrid Electric and Fuel Cell Vehicles”, New York: Third Edition, Chapman and Hall/CRC.

European Tyre & Rubber Manufacturers' Association (2012) “EU Tyre Labelling Regulation 1222/2009,” Version 4.

Fotouhi A., Auger D. J., Propp K., Longo S. (2016a) “Accuracy Versus Simplicity in Online Battery Model Identification”, IEEE Transactions on Systems, Man, and Cybernetics: Systems.

Fotouhi A., Auger D. J., Propp K., Longo S., Wild M. (2016b) “A review on electric vehicle battery modelling: From Lithium-ion toward Lithium-Sulphur”, *Renewable and Sustainable Energy Reviews,* vol. 56, pp. 1008-1021.

Fotouhi A, Auger D. J., O’Neill L., Cleaver T., Walus S. (2017a) “Lithium-Sulfur Battery Technology Readiness and Applications – A Review,” Energies, vol. 10, no. 12, p. 1937.

Fotouhi A., Auger D.J., Propp K., Longo S. (2017b) “Electric Vehicle Battery Parameter Identification and SOC Observability Analysis: NiMH and Li-S Case Studies”, IET Power Electron, doi:10.1049/iet-pel.2016.0777.

Fotouhi A., Auger D.J., Propp K., Longo S. (2017c) “Lithium-Sulfur Battery State-of-Charge Observability Analysis and Estimation”, IEEE Trans. Power Electron., doi:10.1109/TPEL.2017.2740223.

Gerald C., (2016) “Electric Buses in London,” UK eBUS Summit. Low Carbon Vehicle Partnership. Transport for London, London.

Ghaznavi M., Chen P. (2014) “Sensitivity analysis of a mathematical model of lithium-sulfur cells part I”, J. Power Sources, 257, 394–401.

Ghaznavi M., Chen P. (2014) “Sensitivity analysis of a mathematical model of lithium-sulfur cells part II”, J. Power Sources, 257, 402–411.

Gowtham Raj S., Mahesh Kumar S., Sakthivel C., Tamilmaran R., Saravanan B., Kondusamy V. (2016) “Analysis on Bus Body Aerodynamics & Fuel Efficiency in City Buses”, International Journal of Engineering Science and Computing , vol. 6, no. 12, pp. 3788-3793.

Hagen M., Fanz P., Tübke J. (2014) “Cell energy density and electrolyte/sulfur ratio in Li–S cells”, J. Power Sources, 264, 30–34.

Hagen M., Hanselmann D., Ahlbrecht K., Maça R., Gerber D., Tübke J. (2015) “Lithium-sulfur cells: The Gap between the state-of-the-art and the requirements for high energy battery cells. Adv. Energy Mater., 5, 1401986.

Hofmann A.F., Fronczek D.N., Bessler W.G. (2014) “Mechanistic modeling of polysulfide shuttle and capacity loss in lithium-sulfur batteries”, J. Power Sources, 259, 300–310.

Hunt I., Patel Y., Szczygielski M., Kabacik L., Offer G. (2015) “Lithium sulfur battery nail penetration test under load”, J. Energy Storage, 2, 25–29, ISSN 2352-152X, doi:10.1016/j.est.2015.05.007.

Hwang J., Kong K. C., Chang W., Jo E., Nam K., Kim J. (2017) “New liquid carbon dioxide based strategy for high energy/power density LiFePO4”, Nano Energy 36: 398-410.

Irizar (2015) “The Irizar i2e, a 100% Electric bus from the Irizar Group, present in the framework of the Paris Bus COP21”, Ormaiztegi.

Itani K., De Bernardinis A., Khatis Z., Jammal A. (2017) “Comparative analysis of two hybrid energy storage systems used in two front wheel driven electric vehicle during extreme start-up and regenerative braking operations,” *Energy Conversion and Management,* no. 144, pp. 69-87.

Li C., Zhang H., Otaegui L. (2016) “Estimation of energy density of Li-S batteries with liquid and solid Electrolytes”, J. Power Sources, 326, 1–5.

Low Carbon Vehicle Partnership (2018) “Testing & Accreditation - LCEB Certification”, [Online]. Available: https://www.lowcvp.org.uk/initiatives/lceb/lceb-testing.htm. [Accessed 01 05 2018].

Nykvist B., Nilsson M. (2015) “Rapidly falling costs of battery packs for electric vehicles”, *Nature Climate Change,* vol. 5, pp. 329 - 332.

Optare Group Ltd. (2017) “Optare Electric Vehicles,” www.optare.com, Leeds.

OXIS Energy (2018) “19 Ah Rechargeable Ultra Light Lithium Sulfur Pouch Cell,” Abingdon.

OXIS Energy (2019) “Our Cell and Battery Technology Advantages” https://oxisenergy.com/technology/

Piwko M., Kuntze T., Winkler S., Straach S., Härtel P., Althues H., Kaskela S. (2017) “Hierarchical columnar silicon anode structures for high energy density lithium sulfur batteries”, J. Power Sources, 351, 183–191.

Propp K., Marinescu M., Auger D.J., O’Neill L., Fotouhi A., Somasundaram K., Offer G., Minton G., Longo S., Wild M. (2016) “Multi-temperature state-dependent equivalent circuit discharge model for lithium-sulfur batteries”, J. Power Sources, 328, 289–299.

Propp K., Auger D.J., Fotouhi A., Longo S., Knap V. (2017) “Kalman-variant estimators for state of charge in lithium-sulfur batteries”, J. Power Sources, 343, 254–267.

Qnovo: 69. INSIDE THE BATTERY OF A NISSAN LEAF (2015) https://qnovo.com/inside-the-battery-of-a-nissan-leaf/ [Accessed 12 November 2019].

Remy International – BorgWarner (2012) “REMY HVH410-150-DOM Electric Motor Specifications,” Remy International Inc., Pendleton.

Schoemaker J. T. (2007) “Research on the Weight of Buses and Touring Coaches,” International Road Transport Union, Rijswijk.

Stan A. I., Swierczynski M., Store D. I., and Teodorescu R. (2014), “Lithium ion battery chemistries form renewable energy storage to automotive and back-up power applications- an

overview," International conference on optimization of electrical and electronic equipment (OPTIM), Bran, Romania.

Tie S. F., Tan C. W. (2013) "A review of energy sources and energy management system in electric vehicles," *Renewable and Sustainable Energy Reviews,* vol. 20, pp. 82-102.

Varocky B. J. (2011) "Benchmarking of Regenerative Braking for a Fully Electric Car", Eindhoven University of Technology: Report No. D&C 2011.002.

Walus S., Barchasz C., Colin J.F., Martin J.F., Elkaïm E., Leprêtre J.C., Alloin F. (2013) "New insight into the working mechanism of lithium–sulfur batteries: In situ and operando X-ray diffraction characterization", Chem. Commun., 49, 7899–7901.

Walus S., Barchasz C., Bouchet R. (2015) "Lithium/Sulfur Batteries upon Cycling: Structural Modifications and Species Quantification by In Situ and Operando X-ray Diffraction Spectroscopy", Adv. Energy Mater., 5, doi:10.1002/aenm.201500165.

Wild M., O'Neill L., Zhang T., Purkayastha R., Minton G., Marinescu M., Offer G. J. (2015) "Lithium Sulfur batteries, a mechanistic review," *Royal Society of Chemistry,* vol. 8, pp. 3477-3494.

Cranfield University

CERES https://dspace.lib.cranfield.ac.uk

School of Aerospace, Transport and Manufacturing (SATM) Staff publications (SATM)

2020-11-16

How suitable is lithium-sulphur battery for electric city bus application?

Calvo-Serra, Victor

Inderscience

Calvo-Serra VC, Fotouhi A, Soleymani M, Auger DJ. (2020) How suitable is lithium-sulfur battery for electric city bus application? International Journal of Powertrains, Volume 9, Issue 4, October 2020, pp.265-288

https://doi.org/10.1504/IJPT.2020.111227

Downloaded from Cranfield Library Services E-Repository